CONF-790843--4

MASTER

NEUTRAL HYDROGEN FROM THE FOIL-INDUCED DISSOCIATION of $^4HeH^+$, $^3HeH^+$, AND H_2^+

by

Patrick J. Cooney, Donald S. Gemmell, Elliot P. Kanter,
Werner J. Pietsch and Bruce J. Zabransky

Prepared for

8th International Conference
on
Atomic Collisions in Solids
Hamilton, Ontario, Canada
August 13-17, 1979

UofC-AUA-USDOE

ARGONNE NATIONAL LABORATORY, ARGONNE, ILLINOIS

Operated under Contract W-31-109-Eng-38 for the
U. S. DEPARTMENT OF ENERGY

Nucl. Instrum. Methods
Hamilton Conference

NEUTRAL HYDROGEN FROM THE FOIL-INDUCED DISSOCIATION OF $^4HeH^+$, $^3HeH^+$, and H_2^+.*

PATRICK J. COONEY**, DONALD S. GEMMELL, ELLIOT P. KANTER, WERNER J. PIETSCH†, and BRUCE J. ZABRANSKY

Argonne National Laboratory, Argonne, IL 60439

High resolution energy spectra and angular distributions of H^0 from the dissociation of $^4HeH^+$, $^3HeH^+$, and H_2^+ in thin carbon foils are presented for incident ion energies ranging from 170 to 1800 keV/amu. For the range of dwell times inside the target foils studied (about 1 to 10 fsec), the dominant mechanism for such dissociation is the Coulomb explosion of the ions inside the target followed by electron capture near the rear surface of the foil. At the shortest of these dwell times, the yield of H^0 for incident ions oriented perpendicular to the beam relative to that for ions aligned with the beam is a factor of two greater than at longer dwell times. These data indicate that, for ion fragments which emerge from the rear surface of the target within a few angstroms of one another, those in the perpendicular orientation have a greater electron capture probability than those emerging in other orientations.

---

*Work supported by U. S. Department of Energy, Basic Energy Science Division.

**Permanent address: Middlebury College, Middlebury, Vermont.

†Permanent address: University of Cologne, W. Germany.

Considerable information on the interaction of fast-moving ions with matter can be obtained from observing the atomic fragments produced by the dissociation of molecular ions passing through thin foils[1]. The present study considers high-resolution energy spectra and angular distributions for neutral hydrogen (H^o) produced by the dissociation of $^4HeH^+$, $^3HeH^+$, and H_2^+ beams incident on carbon foils having thicknesses ranging from ~100 Å to ~500 Å. Incident-beam kinetic energies ranged from 170 to 725 keV/amu for HeH^+ and 600 to 1800 keV/amu for H_2^+. These measurements represent an extension in incident kinetic energy, incident ion mass, and spectral resolution of previously published data[2]. These data were taken using the Argonne 4-MeV Dynamitron and the associated high-resolution beam line[3].

Figures 1 and 2 show the striking contrast between the joint energy–angular distributions for H^o and H^+ from HeH^+ and H_2^+. One significant difference to be noted is the "dip" on the forward edge of the ring pattern for $HeH^+ \rightarrow H^o$ [fig. 1(b)] in place of the wake-induced peak on the forward edge of the ring pattern for $HeH^+ \rightarrow H^+$ [fig. 2(b)]. A related phenomenon is the existence of "shoulders" on the sides of each H^o ring, when compared to the corresponding H^+ ring. Since the "sides" of these rings correspond to incident ions oriented perpendicular to the beam direction, this suggests an enhanced yield of H^o for such incident ions. The prominent central peak in the $H_2^+ \rightarrow H^o$ ring results from the formation of unbound states of H_2^+ at the rear surface of the foil and their subsequent dissociation into $H^o + H^+$. The latter phenomenon has been examined in a recent publication[4] and will not be discussed here.

One can study the dependence of such ring patterns on the incident ion velocity and on the target foil thickness by examining a pair of single parameter spectra, rather than the complete, two-parameter ring patterns. The energy spectrum of a specific fragment emerging in the forward direction and the corresponding angular distribution at the median fragment energy are sufficient to characterize the size and shape of the ring pattern for that fragment. Representative pairs of such spectra ("crosses") are presented in figs. 3 and 4 for the dissociation of $^4HeH^+$ in carbon foils. Note that, with increasing target thickness (see fig. 4), the separation of each pair of peaks increases and the height of the two peaks in each angular distribution grows smaller, relative to the height of either peak in the corresponding energy spectrum.

Two quantities of interest are the "diameter" of each ring and its "shape". As a measure of the ring "diameter," we use the product of the peak separations, ΔE and $\Delta\theta$, derived from each cross. To first order in v/V,

$$\begin{aligned}\Delta E\Delta\theta &= (2mvV)(2v/V) \\ &= 8\ (mv^2/2) \\ &= 8\ \varepsilon\end{aligned}$$

where ε is the final kinetic energy of the fragment, V is the incident ion's velocity, and v is the fragment's final velocity relative to the center of mass of the molecular ion. A convenient unit for ε is the limiting kinetic energy ε_o which the fragment would have if it experienced a complete Coulomb explosion with an effective product charge $Z_1Z_2e^2$. Thus

$$\varepsilon_o = m_2Z_1Z_2e^2/r_e(m_1 + m_2)$$

where m_1 and m_2 are the masses of the observed and unobserved fragments, respectively, and r_o is their initial separation.

The "shape" of each ring can be characterized by two ratios, namely its back-to-front asymmetry, Y_{L-}/Y_{L+}, and its side-to-front asymmetry, Y_T/Y_{L+}. Y_{L-}, Y_{L+}, and Y_T are, respectively, the peak heights of the low-energy and high-energy peaks in the energy spectrum and the average height of the two peaks in the corresponding angular spectrum.

We may parameterize these data in terms of the ion's dwell time τ inside the foil, expressed in units of a characteristic time τ_o for the dissociation process. We take

$$\tau_o = (\mu r_0^3/2Z_1Z_2e^2)^{1/2}$$

where μ is the reduced mass of the two fragments. For example, $\tau_o \cong 1$ fsec for the dissociation of HeH^+.

Figure 5 compares our measured values of $\varepsilon = \Delta E \Delta\theta/8$ with a simple model for $HeH^+ \rightarrow H^o$. The solid curve represents the result of a Coulomb explosion within the foil which is truncated at the rear surface of the foil. For this simple model,

$$\varepsilon(\tau) = \varepsilon_o \left(1 - \frac{r_o}{r(\tau)}\right)$$

where $r(\tau)$ is the distance between the two fragments at a time τ after the Coulomb explosion begins. The data points were fit to this curve by varying

the overall normalization of Z_1Z_2, after factoring out its velocity dependence. The value of Z_1Z_2 obtained in this way was 70% of that obtained from published stopping powers for He and H ions[5]. While this model neglects many details of this process, such as the wake-potential inside the solid and the formation of unbound states of HeH^+ downstream of the foil, it is quite successful in reproducing the overall trend of the data.

The measured ring asymmetries for H^o (open symbols) and H^+ (solid symbols) are presented in fig. 6. The fact that there are no significant differences in the back-to-front asymmetry for H^o and H^+ [fig. 6(a)] suggests that wake-induced alignment does not depend on the final charge state of the fragment. The marked difference in the side-to-front asymmetry between H^o and H^+ [fig. 6(b)] indicates that there is an enhanced probability of electron capture at the rear surface of the foil when two fragments leave the foil simultaneously, side by side.

One of the authors (P.J.C.) wishes to thank the members of the staff at Argonne National Laboratory for the hospitality shown him during a recent research leave spent there.

References

1) Consult the invited papers by J. Remillieux and D. S. Gemmell in this same issue for a survey of recent work in this area.

2) D. S. Gemmell, P. J. Cooney, W. J. Pietsch, A. J. Ratkowski, Z. Vager, B. J. Zabransky, A. Faibis, G. Goldring, and I. Levine, Proceedings of the 7th International Conference on Atomic Collisions in Solids, Moscow, Sept. 19—23, 1977, in press; M. J. Gaillard, J.-C. Poizat and J. Remillieux, Phys. Rev. Lett. 41 (1978) 159; R. Laubert and F. K. Chen, Phys. Rev. Lett. 40 (1978) 174; M. J. Gaillard, J.-C. Poizat, A. Ratkowski, J. Remillieux, and M. Auzas, Phys. Rev. A 16 (1977) 2323; B. T. Meggitt, K. G. Harrison, and J. W. Lucas, J. Phys. B 6 (1973) L362.

3) B. J. Zabransky, P. J. Cooney, D. S. Gemmell and E. P. Kanter, Rev. Sci. Instr., to be published.

4) E. P. Kanter, P. J. Cooney, D. S. Gemmell, K.-O. Groeneveld, W. J. Pietsch, A. J. Ratkowski, and B. J. Zabransky, Phys. Rev. A, in press.

5) J. F. Zeigler, ed., The Stopping and Ranges of Ions in Matter, vol. 3 and 4 (Pergamon Press, 1977).

Figure Captions

Fig. 1. The joint energy-angle distributions ("ring patterns") for neutral hydrogen arising from the dissociation of (a) 3.0-MeV H_2^+ in a 132-Å carbon foil, and (b) 3.63-MeV $^4HeH^+$ in a 144-Å carbon foil.

Fig. 2. Ring patterns for protons from the dissociation of (a) 1.4-MeV H_2^+ in an 88-Å carbon foil, and (b) 3.0-MeV $^4HeH^+$ in a 195-Å carbon foil.

Fig. 3. Energy spectra in the forward direction (left-hand column) and angular distributions at the median fragment energy (right-hand column) for each fragment arising from the dissociation of 3.63-MeV $^4HeH^+$ in a 160-Å carbon foil. Each complementary pair of such distributions for any given fragment is termed a "cross".

Fig. 4. Crosses for H^o arising from 3.63-MeV $^4HeH^+$ bombarding carbon foils with thicknesses of (a) 160, (b) 360, and (c) 520 Å. These data are normalized for equal numbers of incident $^4HeH^+$ ions.

Fig. 5. The kinetic energy, ε, of outgoing H^o from the dissociation of $^4HeH^+$ and $^3HeH^+$ in carbon foils, plotted as a function of the incident ion's dwell time, τ, within the foil target. The solid curve is the result predicted for a simple Coulomb explosion inside the foil only. The data points have been

fitted to this curve by adjusting a single parameter, namely the effective charge for the explosion within the foil. The units ε_o and τ_o are explained in the text.

Fig. 6. The measured (a) back-to-front and (b) side-to-front asymmetry of the ring patterns for outgoing H^o (open symbols) and H^+ (solid symbols) for various incident velocities HeH^+ ions and various thickness carbon foils, plotted versus the relative dwell time inside the target. Note that, in (b), values of $(Y_T/Y_{L+}) > 1$ correspond to a "dip" on the forward edge of the ring pattern, such as in Fig. 1(b). The symbol shapes have the same meaning as in Fig. 5.

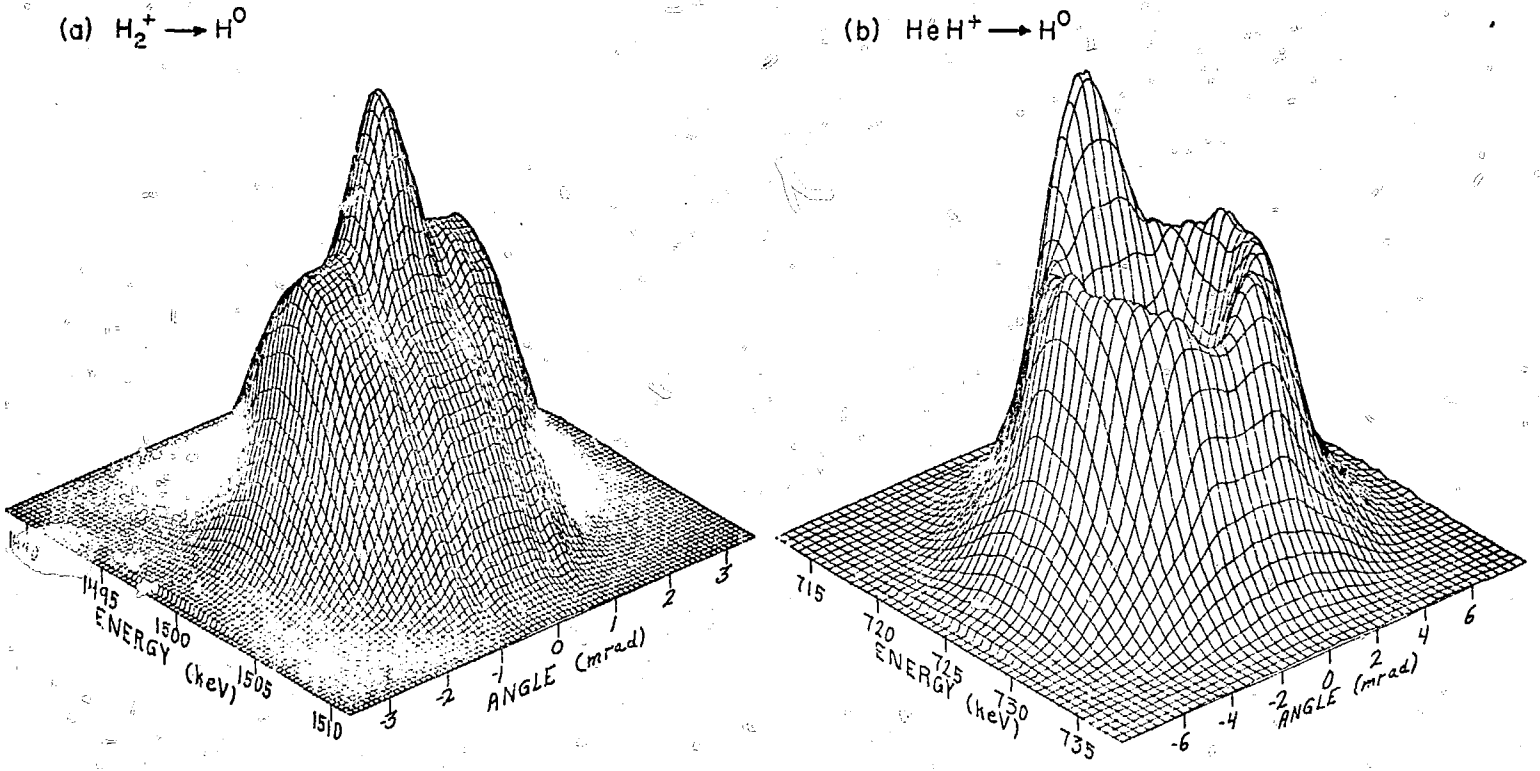
(a) $H_2^+ \longrightarrow H^0$
1495
1500
1505
1510
ENERGY (keV)
-3
-2
-1
0
1
2
3
ANGLE (mrad)
(b) $HeH^+ \longrightarrow H^0$
715
720
725
730
735
ENERGY (keV)
-6
-4
-2
0
2
4
6
ANGLE (mrad)

Figure 1

(a) $H_2^+ \longrightarrow H^+$

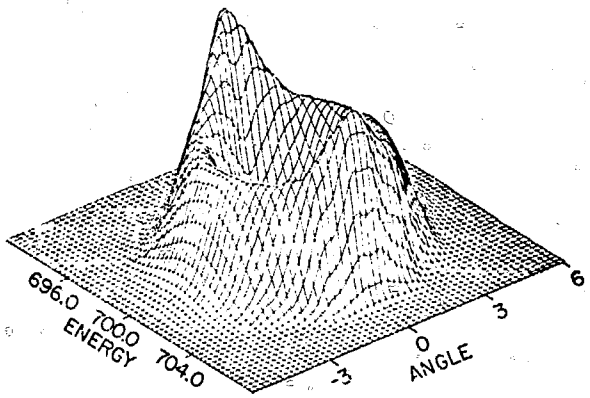

(b) $HeH^+ \longrightarrow H^+$

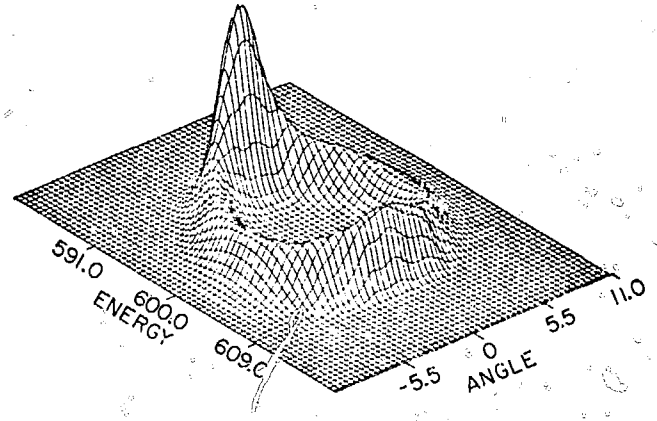

Figure 2

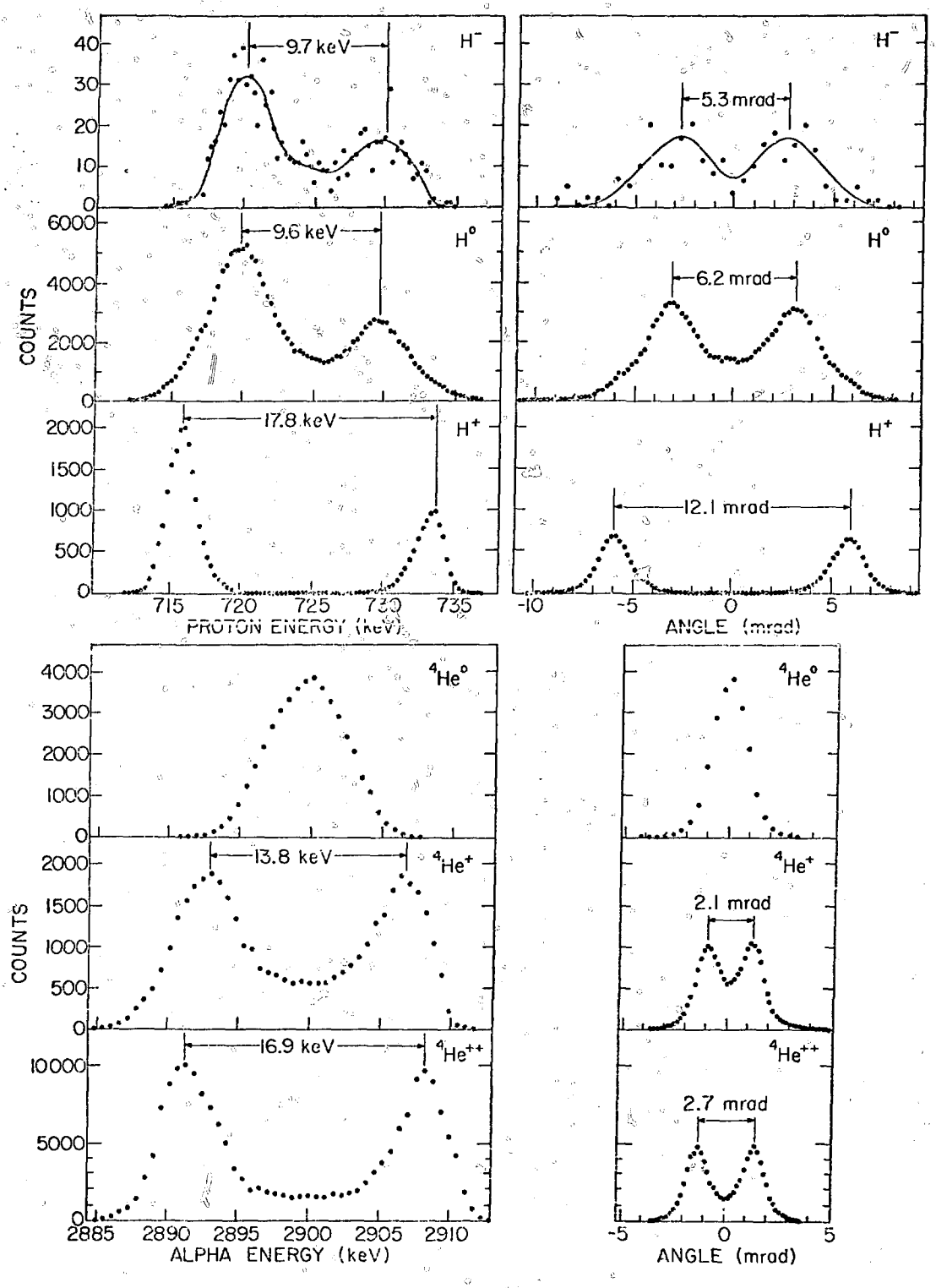
9.7 keV
H⁻
5.3 mrad
9.6 keV
H°
6.2 mrad
17.8 keV
H⁺
12.1 mrad
COUNTS
PROTON ENERGY (keV)
ANGLE (mrad)
⁴He°
13.8 keV
⁴He⁺
2.1 mrad
16.9 keV
⁴He⁺⁺
2.7 mrad
ALPHA ENERGY (keV)

Figure 3

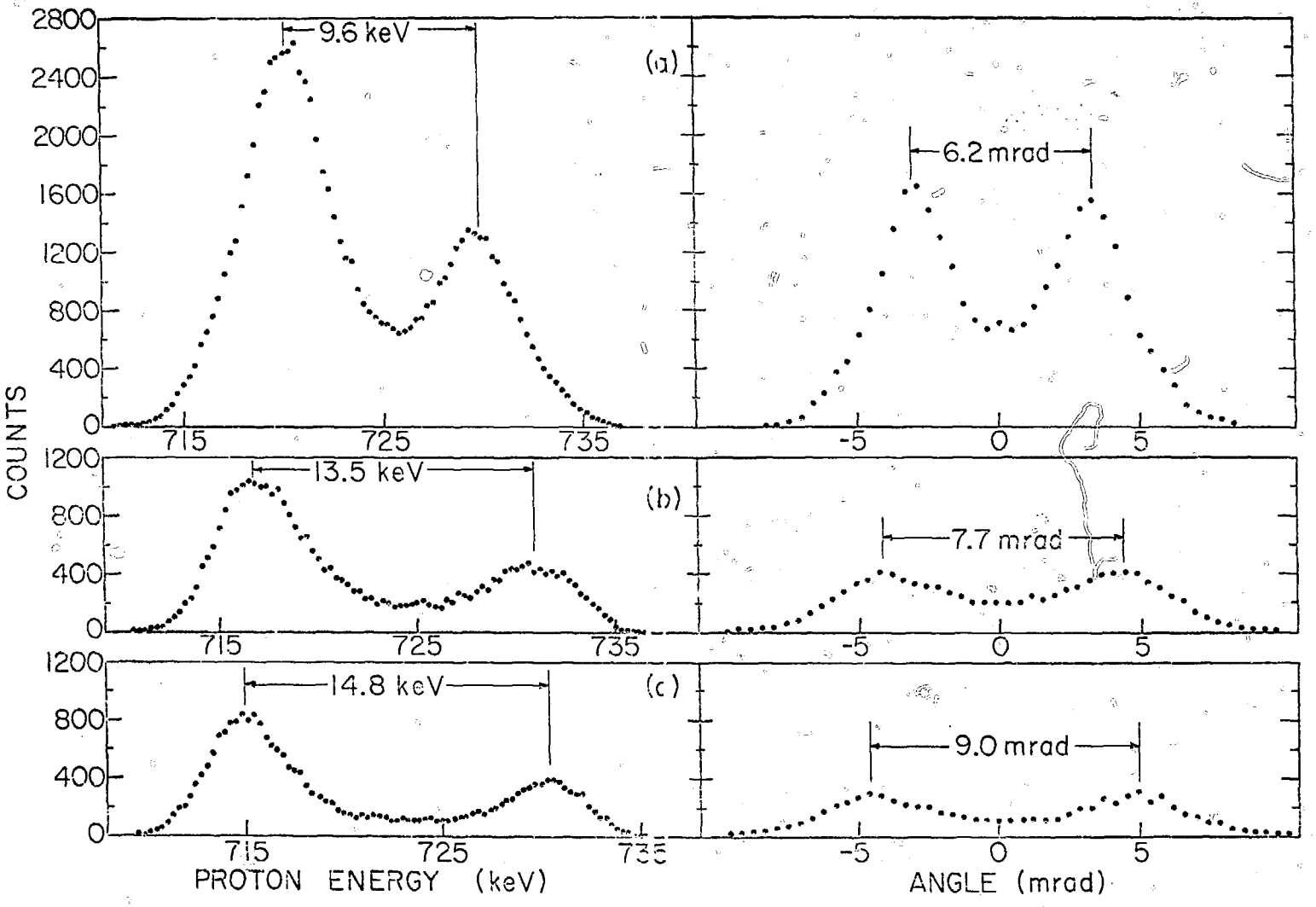
9.6 keV
(a)
6.2 mrad
13.5 keV
(b)
7.7 mrad
14.8 keV
(c)
9.0 mrad
COUNTS
2800
2400
2000
1600
1200
800
400
0
715
725
735
-5
0
5
PROTON ENERGY (keV)
ANGLE (mrad)

Figure 4

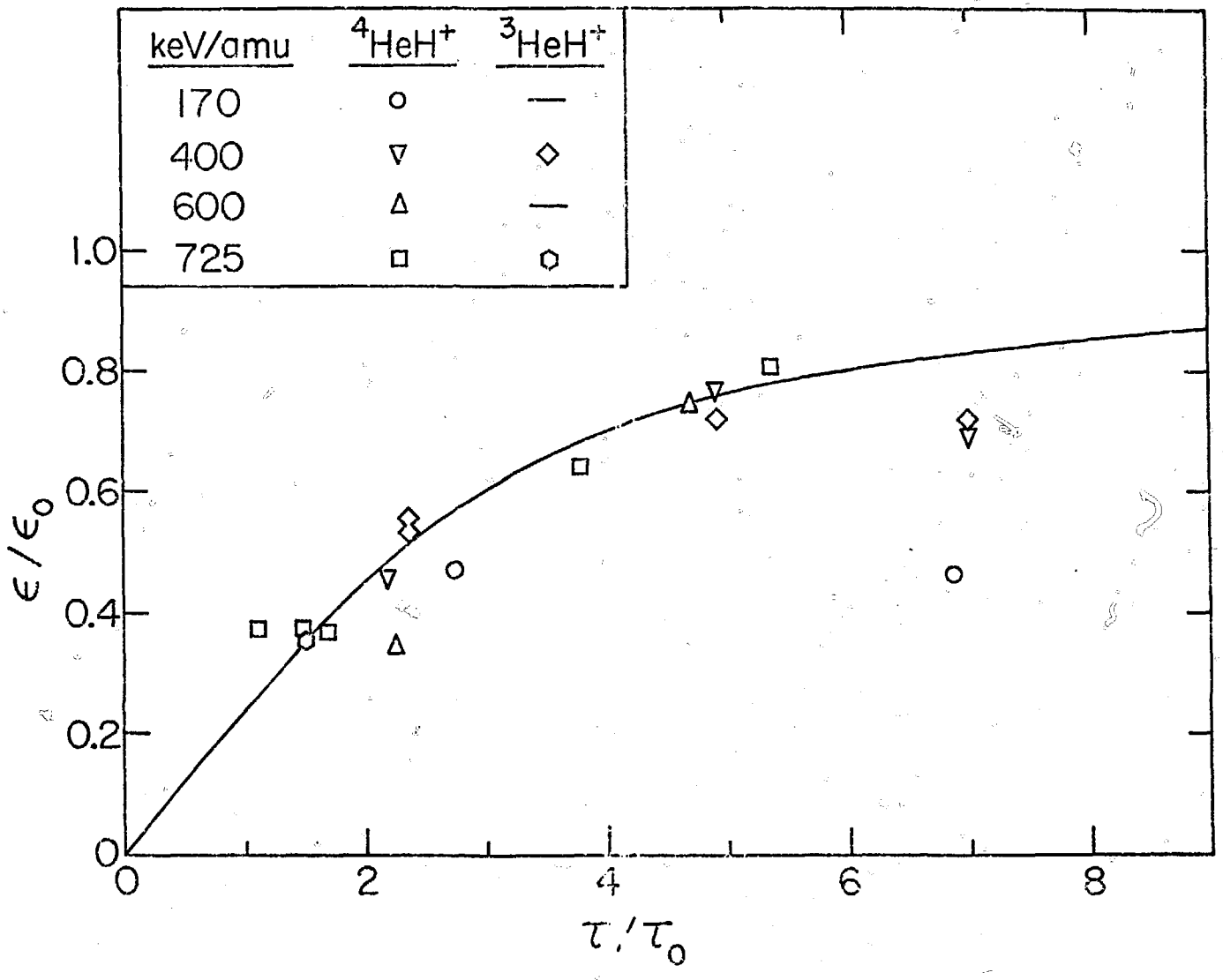
keV/amu
$^4HeH^+$
$^3HeH^+$
170
400
600
725
1.0
0.8
0.6
0.4
0.2
0
ϵ/ϵ_0
0
2
4
6
8
τ'/τ_0

Figure 5

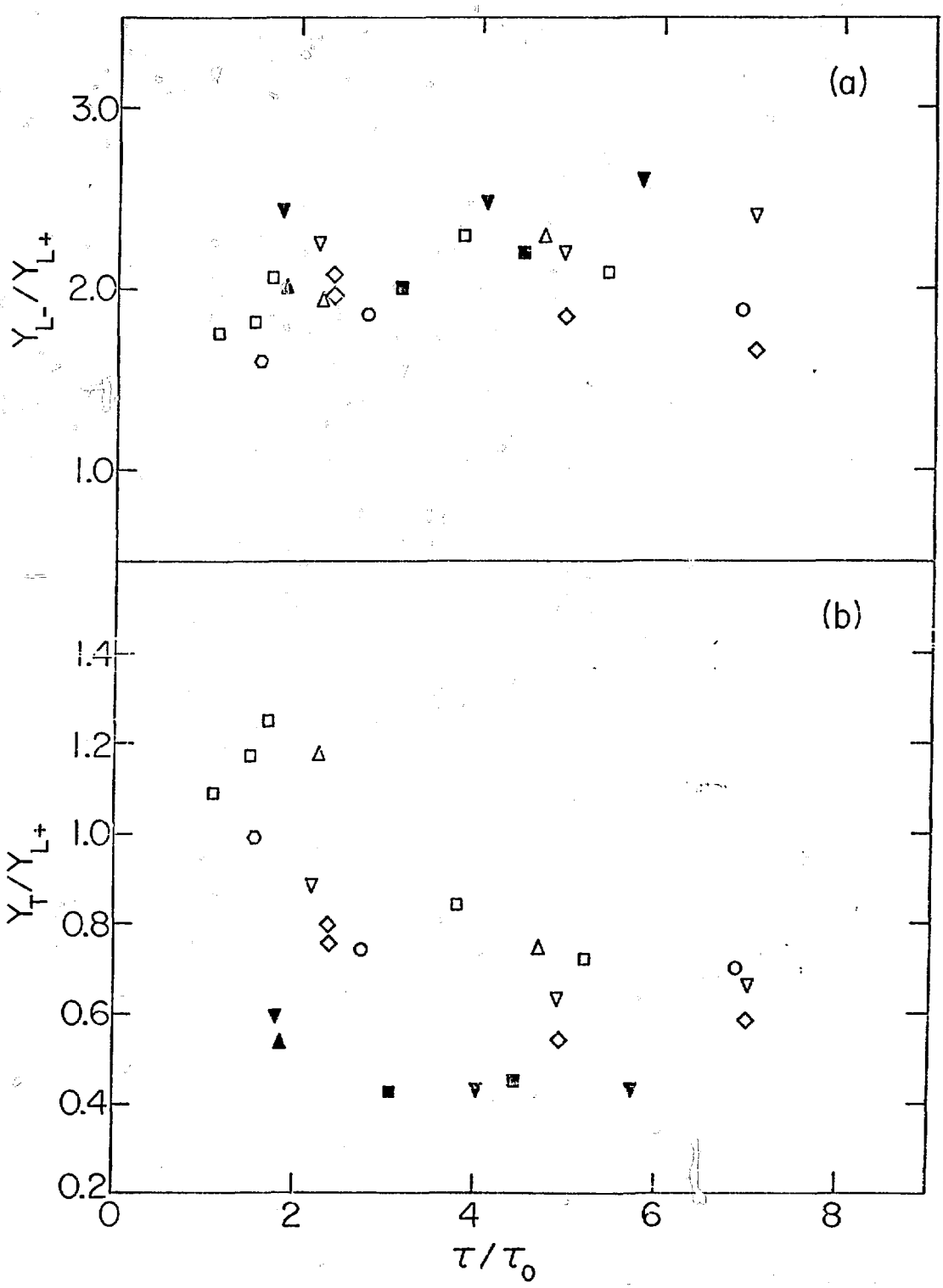

Figure 6